

# Effects of pH and Ionic Strength on the Stability of Nanobubbles in Aqueous Solutions of $\alpha$ -Cyclodextrin

Fan Jin,<sup>†</sup> Junfang Li,<sup>‡</sup> Xiaodong Ye,<sup>‡</sup> and Chi Wu<sup>\*,†,‡</sup>

Department of Chemistry, The Chinese University of Hong Kong, Shatin, N.T., Hong Kong and The Hefei National Laboratory of Physical Science at Microscale, Department of Chemical Physics, The University of Science and Technology of China, Hefei, Anhui 230026, China

Received: June 1, 2007; In Final Form: August 4, 2007

Formation of stable nanobubbles in aqueous solutions of water-soluble organic molecules is a spontaneous process. Using a combination of laser light scattering (LLS) and zeta-potential measurements, we investigated the effects of salt concentration and pH on their stability in  $\alpha$ -cyclodextrin ( $\alpha$ -CD) aqueous solutions. Our results reveal that the nanobubbles are unstable in solution with a higher ionic strength, just like colloidal particles in an aqueous dispersion, but become more stable in alkaline solutions. The zeta-potential measurement shows that the nanobubbles are negatively charged with an electric double layer, presumably due to adsorption of negative OH<sup>-</sup> ions at the gas/water interface. It is this double layer that plays a critical dual role in the formation of stable nanobubbles in aqueous solutions of water-soluble organic molecules, namely, it not only provides a repulsive force to prevent interbubble aggregation and coalescence but also reduces the surface tension at the gas/water interface to decrease the internal pressure inside each bubble.

## Introduction

Most previous experimental and theoretical studies of nanobubbles have focused on a flat macroscopic hydrophobic surface immersed in water or aqueous solution.<sup>1–5</sup> Our previous study shows that the slow relaxation mode observed frequently in aqueous solutions of water-soluble organic molecules is related to formation of stable nanobubbles free in solution, not due to some previously suggested large supramolecules made of water and organic molecules.<sup>6</sup> We developed an effective method to characterize these small bubbles using a combination of laser light-scattering (LLS) and isothermal compressibility measurements. The study of these small bubbles free in solution enables us to investigate the interactions among them, which is not observable at the flat interface. The stabilization of these nanobubbles was attributed to a preferential adsorption of small amphiphilic organic molecules at the gas/water interface. We estimated that the average internal pressure inside each nanobubble is in the range of 2–19 atm because such an adsorbed amphiphilic organic layer reduces the surface tension. However, many questions about these nanobubbles remain unanswered, such as how can they affect the mesoscopic fluid inhomogeneity?<sup>7</sup> What is the stabilization mechanism?<sup>8</sup> How strong is the hydrophobic interaction?<sup>9</sup> How high is the internal pressure?<sup>10</sup> In the current study, we focused on the effects of the ionic strength and pH on the stability of these nanobubbles in an aqueous solution of  $\alpha$ -cyclodextrin.

This study was initially inspired by previous investigations of microbubbles on the macroscopic gas/water interface.<sup>11–16</sup> For example, Marinova et al.<sup>11</sup> found that a macroscopic gas/water interface without any solutes is negatively charged because the hydroxyl ions (OH<sup>-</sup>) from the dissociation–association of water molecules prefers to stay at the gas/water interface. For

small bubbles stable free in aqueous solutions of water-soluble organic molecules, the gas/water interface is mesoscopic. It is natural to ask (1) whether the nanobubbles also have a negatively charged gas/water interface and (2) if so how such negative charges affect their stability. The first question was answered by a combination of LLS and zeta-potential ( $\zeta_{\text{Potential}}$ ) measurements, while the second one was addressed by varying the salt concentration and pH.

## Experimental Section

**Materials and Solution Preparation.**  $\alpha$ -Cyclodextrin ( $\alpha$ -CD, GR from Trade Mark) was purified by recrystallization one time in 60% ethanol aqueous solution and then twice in water. The purified  $\alpha$ -CD was dried in a vacuum oven at 80 °C for ~12 h.<sup>17</sup> Sodium chloride (NaCl, GR from BDH) was heated at ~200 °C for ~2 days to remove organic impurities. Sodium hydroxide (NaOH, GR from UNI-Chem) and hydrochloric acid (HCl, 37% from Fisher) were used without further purification. Water was purified with an inverse osmosis filtration (Nano Pure, Barnstead) until its resistivity reached 18.2 M $\Omega$ ·cm at 20 °C and then filtered with a Millipore PTFE 0.45- $\mu$ m hydrophilic filter. An  $\alpha$ -CD aqueous solution ( $C_{\alpha\text{-CD}} = 7.90 \times 10^{-3}$  g/mL) was prepared at ~20 °C and bubbled by air with a flow rate of ~15 mL/min for 2.5 h to ensure that it was saturated with gas. Note that the nanobubbles can spontaneously form in solution without the air purge. The air purge ensures that each solution studied has the same starting point. To avoid a possible change of the ionic strength or pH, air was pumped through a saturated NaOH aqueous solution to eliminate carbon dioxide (CO<sub>2</sub>) and a Millipore 0.22  $\mu$ m Nylon filter to remove dust particles. The solution pH was adjusted by addition of NaOH or HCl aqueous solution and monitored by a pH meter (ORION 420A). For LLS experiments, each solution was clarified with a Millipore 0.45- $\mu$ m PTFE hydrophilic filter to remove large dust particles.

\* To whom correspondence should be addressed.

<sup>†</sup> The Chinese University of Hong Kong.

<sup>‡</sup> The University of Science and Technology of China.

**Laser Light Scattering.** A commercial LLS instrument (ALV5000) with a vertically polarized 22 mW He–Ne laser head (632.8 nm, Uniphase) was used. The measurable angular range is 15–155°. In our previous study we developed an effective method to analyze both the fast and the slow relaxation modes from each measured intensity–intensity time-correlation function.<sup>6</sup> Further, using a combination of static LLS and statistical thermodynamics,<sup>18,19</sup> we have shown that at a given scattering vector ( $q$ ) the average excess scattering intensities related to the fast and slow modes ( $\langle \Delta I(q) \rangle_{\text{fast}}$  and  $\langle \Delta I(q) \rangle_{\text{slow}}$ ) are, respectively, from small organic molecules free in solution and relatively large nanobubbles with some organic molecules bound at the mesoscopic gas/water interface. At  $q \rightarrow 0$ , we have<sup>6</sup>

$$\langle \Delta I(0) \rangle_{\text{fast}} = K_2 C_f M \quad (1)$$

and

$$\langle \Delta I(0) \rangle_{\text{slow}} = K_1 k_B T \rho_{\text{II}} f \kappa_{\text{T,I}} + \frac{4K_2 f \langle n_b \rangle^2 M^2}{3\pi R_b^3 N_A} \quad (2)$$

where  $N_A$ ,  $k_B$ ,  $T$ ,  $C_f$ , and  $M$  are Avogadro's number, the Boltzmann constant, the absolute temperature, the concentration, and molar mass of small organic molecules free in water, respectively;  $\rho_{\text{II}}$ ,  $\kappa_{\text{T,I}}$ ,  $f$ ,  $\langle n_b \rangle$ , and  $R_b$  are the water density, the isothermal compressibility, the volume fraction, the average number of small organic molecules at the gas/water interface, and the average radius of the nanobubbles, respectively, and  $K_1$  and  $K_2$  are two constants that can be experimentally eliminated. A combination of static and dynamic LLS enables us to determine two corresponding average dynamic correlation lengths ( $\langle \zeta_D \rangle_{\text{fast}}$  and  $\langle \zeta_D \rangle_{\text{slow}}$ ) from<sup>20,21</sup>

$$\langle \Delta I(q) \rangle_{\text{total}} |g^{(1)}(\tau, q)| = \langle \Delta I(q) \rangle_{\text{fast}} e^{-\langle D \rangle_{\text{fast}} q^2 \tau} + \langle \Delta I(q) \rangle_{\text{slow}} e^{-\langle D \rangle_{\text{slow}} q^2 \tau} \quad (3)$$

and

$$\langle \zeta_D \rangle_{\text{fast}} = \frac{k_B T}{3\pi \eta \langle D \rangle_{\text{fast}}} \quad \text{and} \quad \langle \zeta_D \rangle_{\text{slow}} = \frac{k_B T}{3\pi \eta \langle D \rangle_{\text{slow}}} \quad (4)$$

where  $\langle \Delta I(q) \rangle_{\text{total}} (\equiv \langle I(q) \rangle_{\text{solution}} - \langle I(q) \rangle_{\text{water}})$  is the total time-average excess scattering intensity measured in static LLS,  $g^{(1)}(\tau, q)$  is the normalized field–field time-correlation function and can be calculated from the measured intensity–intensity time-correlation function  $G^{(2)}(\tau, q)$  since  $\beta |g^{(1)}(\tau, q)|^2 = [G^{(2)}(\tau, q) - B]/B$  with  $\beta (\leq 1)$  and  $B$  being the optical coherent factor and measured baseline,  $\langle D \rangle$  is the average diffusion coefficient, and  $\eta$  is the solvent viscosity. Further, we can calculate  $R_b$  and  $f$  from  $\langle \zeta_D \rangle_{\text{slow}}$  and  $\langle \Delta I(q) \rangle_{\text{slow}}$ . Note that the average correlation length of the slow mode approximately equals the average diameter of nanobubbles.<sup>6</sup> The scattering angle in the current study was fixed at 20°.

**Electrophoresis/Zeta Potential.** The average mobility ( $\mu_E$ ) of stable nanobubbles under an electric field in an aqueous solution was determined from the frequency shift in a laser Doppler spectrum using a commercial zeta-potential spectrometer (ZetaPlus, Brookhaven) with two platinum-coated electrodes and one He–Ne laser as the light source. Each data point in the mobility measurement was averaged over 40 times at 20 °C. The zeta potential ( $\zeta_{\text{potential}}$ ) can be calculated from  $\mu_E$  using<sup>22</sup>

$$\mu_E = \frac{2\epsilon \zeta_{\text{potential}}}{3\eta} f(\kappa R_b) \quad (5)$$

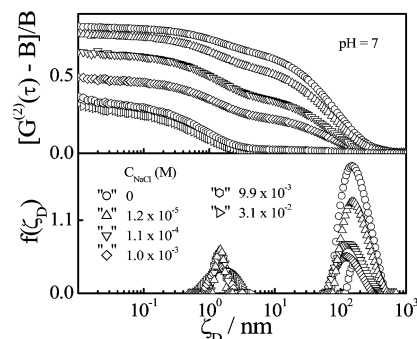


**Figure 1.** Salt concentration dependence of intensity–intensity time correlation functions ( $[G^{(2)}(\tau) - B]/B$ ) of  $\alpha$ -CD neutral aqueous solutions and their corresponding dynamic correlation-length distributions ( $f(\zeta_D)$ ).

where  $\epsilon$  is the permittivity of water and  $1/\kappa$  is the Debye screening length.<sup>23</sup> When  $\kappa R_b \ll 1$  (the Hückel limit),  $f(\kappa R_b) \approx 1$ , and when  $\kappa R_b \gg 1$  (the Smoluchowski limits),  $f(\kappa R_b) \approx 1.5$ .<sup>24</sup> In the current study, the nanobubbles become unstable in solutions with a higher ionic strength. Therefore, it is impossible to keep the ionic strength in the zeta-potential measurements over a wide pH range 2.0–12. Rather than using the Hückel or Smoluchowski limit, we can analyze our data using the Ohshima equation<sup>25</sup>

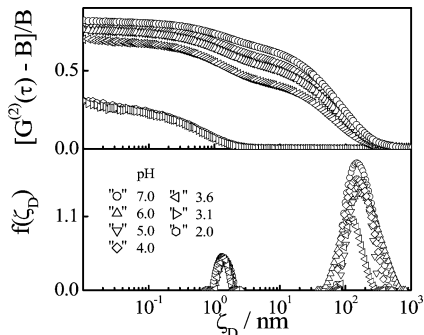
$$f(\kappa R_b) = 1 + \frac{1}{2[1 + \delta/\kappa R_b]^3} \quad (6)$$

to calculate  $\zeta_{\text{potential}}$  over the whole range of  $\kappa R_b$ , where  $2 \leq \delta \leq 3$ , a constant for a given system. The mobility unit used in this study is mU, corresponding to  $10^{-8} \text{ m}^2 \text{ s}^{-1} \text{ V}^{-1}$  in SI units.

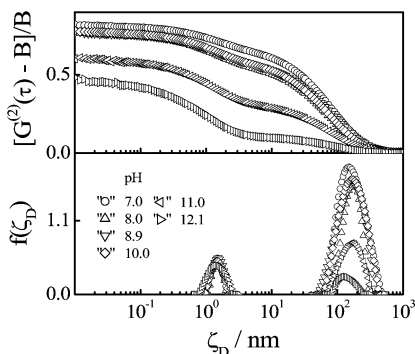
## Results and Discussion

Figure 1 shows typical measured intensity–intensity time-correlation functions  $[G^{(2)}(\tau)]$  of  $\alpha$ -CD aqueous solutions with different amounts of NaCl ( $C_{\text{NaCl}} = 0$ –0.1 M) and their corresponding dynamic correlation length distributions  $f(\zeta_D)$ . Note that we have scaled the x axis of  $G^{(2)}(\tau)$  by  $k_B T q^2 / 3\pi \eta$  so that  $G^{(2)}(\tau)$  can be directly compared with  $f(\zeta_D)$ . Each  $f(\zeta_D)$  is normalized by its corresponding total time-average excess scattering intensity  $\langle \Delta I(q) \rangle_{\text{total}}$ . In this way, peak areas ( $A_{\text{fast}}$  and  $A_{\text{slow}}$ ) of the fast and slow modes are directly related to  $\langle \Delta I(q) \rangle_{\text{fast}}$  and  $\langle \Delta I(q) \rangle_{\text{slow}}$ , respectively. The average dynamic correlation length ( $\langle \zeta_D \rangle_{\text{fast}}$ ) of the fast mode is only  $\sim 1.4$  nm, attributing to individual  $\alpha$ -CD molecules free in the solution, while the slow mode with an average dynamic correlation length ( $\langle \zeta_D \rangle_{\text{slow}}$ ) of  $\sim 160$  nm is related to relatively large nanobubbles. It is clear that as  $C_{\text{NaCl}}$  increases,  $A_{\text{fast}}$  nearly remains constant but  $A_{\text{slow}}$  decreases. When  $C_{\text{NaCl}} \geq \sim 0.02$  M, the slow mode completely vanishes, revealing that addition of salt can destabilize the nanobubbles. Such a salt-out phenomena is well known in colloidal science because addition of salt increases the ionic strength and reduces the thickness ( $1/\kappa$ ) of the electric double layer so that there is no sufficient repulsive force to stabilize colloidal particles.<sup>23</sup> On the other hand, the effect of salt on  $A_{\text{fast}}$  is much lower, suggesting that most of the  $\alpha$ -CD molecules are free in solution and only a very small amount are adsorbed at the gas/water interface.

Figure 2 shows no significant change in both  $A_{\text{slow}}$  and  $\langle \zeta_D \rangle_{\text{slow}}$  in the range  $4 \leq \text{pH} \leq 7$ . When  $\text{pH} \leq 4$ , the peak attributed to the slow mode becomes smaller as pH decreases and completely vanishes at  $\text{pH} < 3$ . It clearly indicates that the nanobubbles are unstable in acidic solutions. While in alkaline



**Figure 2.** pH dependence of intensity–intensity time correlation functions ( $[G^{(2)}(\tau) - B]/B$ ) of  $\alpha$ -CD aqueous solutions under acidic conditions and their corresponding dynamic correlation-length distributions ( $f(\zeta_D)$ ).



**Figure 3.** pH dependence of intensity–intensity time correlation functions ( $[G^{(2)}(\tau) - B]/B$ ) of  $\alpha$ -CD aqueous solutions under alkaline conditions and their corresponding dynamic correlation-length distributions ( $f(\zeta_D)$ ).

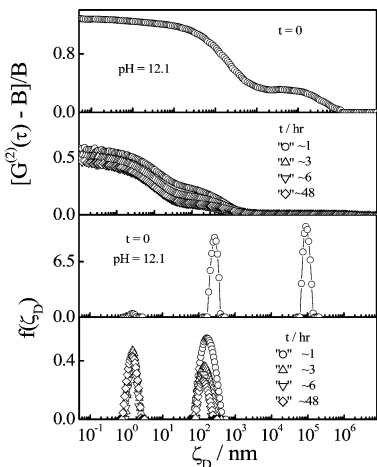


**Figure 4.** Time dependence of intensity–intensity time correlation functions ( $[G^{(2)}(\tau) - B]/B$ ) of an  $\alpha$ -CD solution at a higher pH and their corresponding dynamic correlation-length distributions ( $f(\zeta_D)$ ).

solutions,  $A_{\text{slow}}$  nearly remains constant in the range  $7 \leq \text{pH} \leq 10$  as shown in Figure 3. Further increase of pH leads to a decrease of  $A_{\text{slow}}$  but not to zero even at  $\text{pH} > 12$ . A combination of Figures 2 and 3 shows that for a given ionic strength, the nanobubbles are more stable under alkaline condition. It should be stated that immediately after adjusting the pH to  $\sim 12$ , we observed an additional ultra-slow relation mode with a correlation length longer than  $\sim 100 \mu\text{m}$ , as shown in Figure 4. Note that this ultra-slow mode disappears after  $\sim 1$  h. Figure 4 also shows that  $A_{\text{slow}}$  with its peak located at  $\sim 100$  nm decreases with increasing time and reaches its equilibrium after  $\sim 6$  h. Presumably, this additional ultra-slow mode is due to the existence of some unstable microbubbles generated from the

**TABLE 1: Salt Concentration and pH Dependence of Average Dynamic Lengths ( $\langle \zeta_D \rangle_{\text{fast}}$  and  $\langle \zeta_D \rangle_{\text{slow}}$ ) of Fast and Slow Relaxation Modes of  $\alpha$ -CD Aqueous Solutions and Their Related Time-Average Excess Scattering Intensities ( $\langle \Delta I(q) \rangle_{\text{fast}}$  and  $\langle \Delta I(q) \rangle_{\text{slow}}$ )**

$C_{\text{NaCl}}$ (M), where pH = 7.0	$\langle \zeta_D \rangle_{\text{fast}}/\text{nm}$	$\langle \Delta I(q) \rangle_{\text{fast}}$	$\langle \zeta_D \rangle_{\text{slow}}/\text{nm}$	$\langle \Delta I(q) \rangle_{\text{slow}}$
0	1.4	0.13	162	0.92
$1.2 \times 10^{-6}$	1.4	0.13	158	0.85
$1.2 \times 10^{-5}$	1.4	0.13	160	0.71
$3.1 \times 10^{-5}$	1.4	0.14	158	0.63
$1.1 \times 10^{-4}$	1.4	0.14	154	0.34
$1.0 \times 10^{-3}$	1.4	0.14	164	0.24
$4.8 \times 10^{-3}$	1.4	0.14	170	0.11
$9.9 \times 10^{-3}$	1.4	0.13	152	0.04
$3.1 \times 10^{-2}$	1.4	0.14	no slow mode	0
$1.0 \times 10^{-2}$	1.4	0.14	no slow mode	0
$2.5 \times 10^{-2}$	1.4	0.14	no slow mode	0

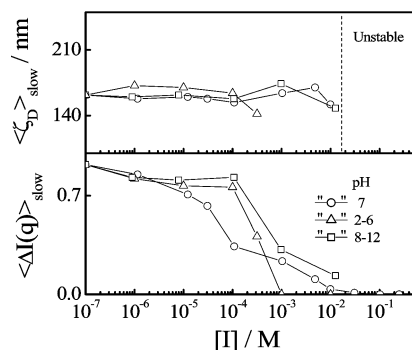
  

pH, where $C_{\text{NaCl}} = 0$	$\langle \zeta_D \rangle_{\text{fast}}/\text{nm}$	$\langle \Delta I(q) \rangle_{\text{fast}}$	$\langle \zeta_D \rangle_{\text{slow}}/\text{nm}$	$\langle \Delta I(q) \rangle_{\text{slow}}$
2.0	1.4	0.13	no slow mode	0
3.1	1.4	0.13	no slow mode	0
3.6	1.4	0.13	142	0.41
4.0	1.4	0.14	164	0.76
5.0	1.4	0.14	170	0.77
6.0	1.4	0.14	172	0.82
7.0	1.4	0.13	162	0.92
8.0	1.4	0.13	160	0.83
8.9	1.4	0.13	162	0.81
10.0	1.4	0.13	158	0.83
11.0	1.4	0.14	174	0.32
12.1 after $\sim 48$ h	1.4	0.13	150	0.12

nanobubble coalescence, which also explains the decrease of  $A_{\text{slow}}$  because some nanobubbles are merged into large microbubbles that eventually float out of the solution.

It is helpful to note that addition of NaOH in the adjustment of pH has two opposite effects on formation of stable nanobubbles. On one hand, adsorption of more  $\text{OH}^-$  ions increases negative charges at the gas/water interface and stabilizes the nanobubbles. On the other hand, it increases the ionic strength of the solution and reduces the effective interbubble repulsive force so that the nanobubbles can undergo aggregation and coalescence. Our results reveal that adsorption of more  $\text{OH}^-$  ions is dominant, so that for a given ionic strength, the nanobubbles are much more stable under alkaline conditions. Table 1 summarizes the salt concentration and pH dependence of  $\langle \zeta_D \rangle_{\text{fast}}$ ,  $\langle \zeta_D \rangle_{\text{slow}}$ ,  $\langle \Delta I(q) \rangle_{\text{fast}}$ , and  $\langle \Delta I(q) \rangle_{\text{slow}}$ . It shows that both the ionic strength and pH have nearly no effect on  $\langle \zeta_D \rangle_{\text{fast}}$  and  $\langle \Delta I(q) \rangle_{\text{fast}}$ , which is expected because  $\alpha$ -CD has a constant size and most of them are free in the solution. Moreover,  $\langle \zeta_D \rangle_{\text{slow}}$  is also nearly independent of  $C_{\text{NaCl}}$  and pH, indicating that stable nanobubbles have a constant average size.

Figure 5 summarizes  $\langle \zeta_D \rangle_{\text{slow}}$  and  $\langle \Delta I(q) \rangle_{\text{slow}}$  under different conditions. In a neutral solution,  $\langle \Delta I(q) \rangle_{\text{slow}}$  decreases as the ionic strength ( $[I]$ ) increases and vanishes when  $[I] > \sim 0.02$  M, but  $\langle \zeta_D \rangle_{\text{slow}}$  nearly remains constant ( $\sim 160$  nm) in the range  $10^{-7} \leq [I] \leq 10^{-2}$  M. In acidic solutions,  $\langle \Delta I(q) \rangle_{\text{slow}}$  nearly remains constant in the range  $10^{-7} \leq [I] \leq 10^{-4}$  M but significantly decreases as  $[I]$  further increases and even approaches zero when  $[I] > \sim 10^{-3}$  M. Note that for a similar ionic strength ( $\sim 10^{-3}$  M),  $\langle \Delta I(q) \rangle_{\text{slow}}$  is still finite in neutral or alkaline solutions. Therefore, formation of stable nanobubbles in acidic solution is unfavorable. On the other hand,  $\langle \zeta_D \rangle_{\text{slow}}$  remains  $\sim 160$  nm in the range  $10^{-7} \leq [I] \leq 10^{-4}$  M and only slightly decreases to 140 nm when  $[I]$  increases to  $3 \times 10^{-4}$



**Figure 5.** Ionic strength ( $[I]$ ) dependence of slow-mode-related time-average excess scattering intensity ( $\langle \Delta I(q) \rangle_{\text{slow}}$ ) of  $\alpha$ -CD aqueous solutions under different pH conditions and the corresponding average dynamic correlation lengths ( $\langle \zeta_D \rangle_{\text{slow}}$ ).

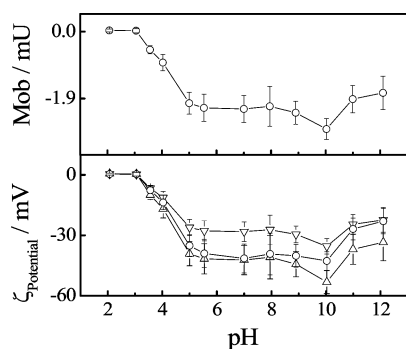


**Figure 6.** pH dependence of average mobility ( $\mu_E$ ) and its corresponding zeta potential ( $\zeta_{\text{potential}}$ ) calculated under different limiting conditions: ( $\nabla$ ) Smoluchowski, ( $\Delta$ ) Hückel, and ( $\circ$ ) Ohshima.

M. In alkaline solutions,  $\langle \Delta I(q) \rangle_{\text{slow}}$  also remains constant in the range  $10^{-7} \leq [I] \leq 10^{-4}$  M but significantly decreases as  $[I]$  further increases. While in alkaline solutions,  $\langle \Delta I(q) \rangle_{\text{slow}}$  remains finite even at  $[I] \approx 10^{-2}$  M. The constant  $\langle \zeta_D \rangle_{\text{slow}}$  over the entire range  $10^{-7} \leq [I] \leq 10^{-2}$  M reveals that stable nanobubbles have a properly controlled size.

Zhang et al.<sup>4</sup> have not detected any significant difference in the stability or morphology of nanobubbles on a surface upon addition of electrolytes. Our results clearly indicate that addition of electrolytes can affect the stability of the nanobubbles in solutions. Such a difference could be attributed the surface effect. Namely, in solution the nanobubbles are free and randomly diffuse inside due to thermal agitation. Addition of electrolytes reduces the repulsion force among the nanobubbles, so that they can aggregate and merge together to form larger bubbles. In contrast, on a surface the nanobubbles are fixed and less mobile, so that their aggregation is suppressed.

Figure 6 shows the pH dependence of the average mobility ( $\mu_E$ ) of the nanobubbles under an electric field in aqueous solutions as well as their corresponding zeta potentials ( $\zeta_{\text{potential}}$ ) calculated under different limiting conditions. Under the Ohshima equation,  $\zeta_{\text{potential}}$  is  $-40$  mV in the range  $5.5 \leq \text{pH} \leq 10$ , revealing that the nanobubbles are negatively charged. The decrease of pH from 5.0 to 3.0 leads to a change of  $\zeta_{\text{potential}}$  from  $-40$  mV to 0. It clearly shows that the increase of proton concentration not only increases the ionic strength and reduces the thickness of the electric double layer but also neutralizes the negatively charged gas/water interface and destabilizes the nanobubbles. Further, as pH decreases, the averaged size of the nanobubbles slightly decreases from  $\sim 160$  to  $\sim 140$  nm, but the zeta potential changes from  $-40$  to  $-10$  mV. It implies that the surface tension is mainly reduced by adsorption of amphiphilic  $\alpha$ -CD molecules at the gas/water interface and that

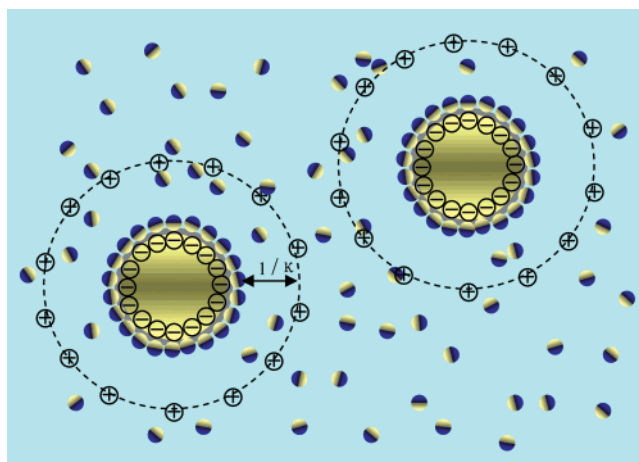


**Figure 7.** Schematic of stable nanobubbles in an aqueous solution of small amphiphilic water-soluble organic molecules that are represented by  $\bullet$ .

even the intrabubble electrostatic repulsive force generated by the adsorbed negative  $\text{OH}^-$  ions also reduces the surface tension. Therefore, the pressure difference between the inside and outside of each nanobubbles ( $\Delta P$ ) can be estimated by a modified Laplace–Young equation

$$\Delta P + P_{\text{Maxwell}} = \frac{2\gamma}{R_b} \quad (7)$$

where  $P_{\text{Maxwell}}$  is the additional Maxwell pressure generated from the intrabubble electrostatic repulsion and  $\gamma$  is the surface tension at the gas/water interface. Note that the average size of the nanobubbles nearly remains a constant, implying that the contribution of  $P_{\text{Maxwell}}$  to the reduction of surface tension is relatively small. Previously, we estimated that the internal pressure is in the range of 2–19 atm by only considering adsorption of a layer of small amphiphilic water-soluble organic molecules at the gas/water interface. Previously, Zhang et al.<sup>4</sup> estimated that the surface tension ( $\gamma$ ) of the nanobubbles attached on a surface in a surfactant solution was reduced to  $\sim 20$ – $40$  mN/m<sup>-1</sup>, so that the minimal internal pressure should be  $\sim 4$  atm for a nanobubbles with a size of  $\sim 100$  nm. Their results suggest that the contribution of  $P_{\text{Maxwell}}$  can be ignored for individual nanobubbles attached on a surface. Our current results suggest that the internal pressure could be even lower due to the existence of an additional Maxwell pressure generated by negatively charged  $\text{OH}^-$  ions at the interface.

## Conclusion

Both salt and pH can influence formation of stable nanobubbles in aqueous solutions of  $\alpha$ -cyclodextrin ( $\alpha$ -CD). A combination of laser light scattering (LLS) and zeta-potential measurements reveals that the gas/water interface of each nanobubble is negatively charged with an electric double layer. Just like colloidal particles, the nanobubbles can also be salted out, namely, an increase of the ionic strength (salt concentration) reduces the double-layer thickness and destabilizes the nanobubbles. For a given ionic strength, the nanobubbles are more stable in alkaline solution because the adsorption of more  $\text{OH}^-$  ions at the gas/water interface enhances the double layer. A structural model is proposed for stable nanobubbles in which not only small amphiphilic water-soluble organic molecules but also negatively charged  $\text{OH}^-$  ions are adsorbed at the gas/water interface, as shown in Figure 7. Both stabilize the nanobubbles and prevent coalescence. The charged interface generates an

additional Maxwell pressure and further decreases the surface tension, so that the pressure inside each nanobubble is further reduced. This provides a better explanation of why the nanobubbles with a huge surface area are still stable in aqueous solutions of various water-soluble low molar mass organic molecules.

**Acknowledgment.** The financial support of the Chinese Academy of Sciences (CAS) Special Grant (KJCX2-SW-H14), the National Natural Scientific Foundation of China (NNSFC) Projects (20534020 and 20574065), and the Hong Kong Special Administration Region (HKSAR) Earmarked Project (CU-HK4025/04P, 2160242) is gratefully acknowledged.

## References and Notes

- (1) Tyrrell, J. W. G.; Attard, P. *Phys. Rev. Lett.* **2001**, *87*, 176104–1.
- (2) Ishida, N.; Inoue, T.; Miyahara, M.; Higashitani, K. *Langmuir* **2000**, *16*, 6377.
- (3) Considine, R. F.; Drummond, C. J. *Langmuir* **2000**, *16*, 631.
- (4) Zhang, X. H.; Nobuo, M.; Craig, V. S. J. *Langmuir* **2006**, *22*, 5025.
- (5) Zhang, X. H.; Zhang, X. D.; Lou, S. T.; Zhang, Z. X.; Sun J. L.; Hu, J. *Langmuir* **2004**, *20*, 3813.
- (6) Jin, F.; Ye, J.; Hong, L.; Lam, H.; Wu, C. *J. Phys. Chem. B* **2007**, *111*, 2255.
- (7) Henderson, D. *Fundamentals of Inhomogeneous Fluids*; CRC Press: New York, 1992.
- (8) Lugli, F.; Hofinger, S.; Zerbetto, F. *J. Am. Chem. Soc.* **2005**, *127*, 8020.
- (9) Lum, K.; Chandler, D.; Weeks, J. D. *J. Phys. Chem. B* **1999**, *103*, 4750.
- (10) Ljunggren, S.; Reiksson, J. C. *Colloids Surf. A* **1997**, *151*, 129.
- (11) Marinova, K. G.; Alargova, R. G.; Denkov, N. D.; Velev, O. D.; Petsev, D. N.; Ivanov, I. B.; Borwankar, R. P. *Langmuir* **1996**, *12*, 2045.
- (12) Craig, V. S. J.; Ninham, B. W.; Pashley, R. M. *J. Phys. Chem.* **1993**, *97*, 10192.
- (13) Hanweright, J.; Zhou, J.; Evans, G. M.; Galvin, K. P. *Langmuir* **2005**, *21*, 4912.
- (14) Kim, J. Y.; Song, M. G.; Kim, J. D. *J. Colloid. Interface Sci.* **2000**, *223*, 285.
- (15) Cho, S. H.; Kim, J. Y.; Chun, J. H.; Kim, J. D. *Colloids Surf. A* **2005**, *269*, 28.
- (16) Saulnier, P.; Bouriart, P.; Morel, G.; Lachaise, J.; Graciaa, A. *J. Colloid Interface Sci.* **1998**, *200*, 81.
- (17) Armstrong, D. W.; Nome, F.; Spino, L. A.; Golden, T. D. *J. Am. Chem. Soc.* **1986**, *108*, 1418.
- (18) Brown, W. *Light Scattering*; Clarendon Press: Oxford, 1996.
- (19) Plischke, M.; Bergersen, B. *Equilibrium Statistical Physics*, 2nd ed; World Scientific: River Edge, NJ, 1994.
- (20) Berne, B.; Pecora, R. *Dynamic Light Scattering*; Plenum Press: New York, 1976.
- (21) Chu, B. *Laser Light Scattering*, 2nd ed.; Academic Press: New York, 1991.
- (22) Hunter, R. J. *Zeta Potential in Colloid Science*; Academic Press: London, 1981.
- (23) Hunter, R. J. *Foundations of Colloid Science*, 2nd ed.; Oxford Press: Oxford, 2000.
- (24) Henry, D. C. *Proc. R. Soc.* **1931**, *A133*, 106.
- (25) Ohshima, H. *J. Colloid Interface Sci.* **1994**, *168*, 269.